Final Report

NASA Cooperative Agreement NCC-1-273

CONTROL DESIGN STRATEGIES TO ENHANCE LONG-TERM AIRCRAFT STRUCTURAL INTEGRITY

By

Dr. Brett A. Newman, Principal Investigator
Department of Aerospace Engineering

Submitted by

Old Dominion University
Research Foundation
800 West 46th Street
Norfolk, VA 23508

June 1999

!

Summary Report for NCC-1-273
Control Design Strategies To Enhance Long-Term Aircraft Structural Integrity

Over the operational lifetime of both military and civil aircraft, structural components are exposed to hundreds of thousands of low-stress repetitive load cycles and less frequent but higher-stress transient loads originating from maneuvering flight and atmospheric gusts. Micro-material imperfections in the structure, such as cracks and debonded laminates, expand and grow in this environment, reducing the structural integrity and shortening the life of the airframe. Extreme costs associated with refurbishment of critical load-bearing structural components in a large fleet, or altogether reinventoring the fleet with newer models, indicate alternative solutions for life extension of the airframe structure are highly desirable. Increased levels of operational safety and reliability are also important factors influencing the desirability of such solutions.

One area having significant potential for impacting crack growth/fatigue damage reduction and structural life extension is flight control. To modify the airframe response dynamics arising from command inputs and gust disturbances, feedback loops are routinely applied to vehicles. A dexterous flight control system architecture senses key vehicle motions and generates critical forces/moments at multiple points distributed throughout the airframe to elicit the desired motion characteristics. In principle, these same control loops can be utilized to influence the level of exposure to harmful loads during flight on structural components. Project objectives are to investigate and/or assess the leverage control has on reducing fatigue damage and enhancing long-term structural integrity, without degrading attitude control and trajectory guidance performance levels. In particular, efforts have focused on the effects inner loop control parameters and architectures have on fatigue damage rate. To complete this research, an actively controlled flexible aircraft model and a new state space modeling procedure for crack growth have been utilized.

Analysis of the analytical state space model for crack growth revealed the critical mathematical factors, and hence the physical mechanism they represent, that influenced high rates of airframe crack growth. The crack model was then exercised with simple load inputs to uncover and expose key crack growth behavior. To characterize crack growth behavior, both "short-term" laboratory specimen test type inputs and "long-term" operational flight type inputs were considered. Harmonic loading with a single overload revealed typical exponential crack growth behavior until the overload application, after which time the crack growth was retarded for a period of time depending on the overload strength. An optimum overload strength was identified which leads to maximum retardation of crack growth. Harmonic loading with a repeated overload of varying strength and frequency again revealed an optimum overload trait for maximizing growth retardation. The optimum overload strength ratio lies near the range of 2 to 3 with dependency on frequency. Experimental data was found to correlate well with the analytical predictions.

A flexible aircraft dynamic model and the modeling procedure is presented and analyzed. A specific numerical model is given and its characteristics are noted. Poor flight dynamic characteristics are indicated and a nominal inner loop flight control system are designed to correct these deficiencies. The control system was not designed to directly influence crack growth behavior. An approximate stress model for an internal structural component of the aircraft was developed. The structural component is representative of a fuselage skin stiffener undergoing bending. The stress model relies heavily upon the structural dynamics model imbedded within the overall aircraft model, and in particular on deflection mode shapes, frequencies and dampings.

Even though the feedback system was not specifically designed to control stress in this or any other structural component, the control system allowed for an improvement in reducing stress transients during vehicle maneuvers, relative to similar open-loop responses. The vehicle motions were excited by both stick commands and atmospheric turbulence.

Integration of the flexible aircraft model (open-loop and closed-loop cases) with the fatigue crack growth model was considered to address the overall research objectives. The stress output from the aircraft model serves as the input to the crack growth model. A matrix of simulation test cases was constructed to cover such variables as open-loop operation, nominal closed-loop operation, perturbed closed-loop operation (i.e., feedback gain variations), nominal maneuver profile, perturbed maneuver profile (including overload strength and frequency), atmospheric gust, and mean stress level. Simulation output data including crack length vs. number of load cycles is used to predict long-term structural integrity, and more importantly to expose the important factors influencing this integrity. Results indicate feedback control can provide significant leverage on crack growth. Large percentage improvements in structural life were predicted. Feedback gains associated with structural mode suppression loops were determined to be particularly influential in affecting crack growth. Results also indicate existence of nonintuitive optimal overload strength and frequency values which minimize crack growth. Cases exist where higher overloads reduce crack growth. This result has important implication for designing new control logic which exploits this behavior.

The NCC-1-273 grant supported one Master of Science (M.S.) graduate student in the Department of Aerospace Engineering, Old Dominion University. The student was Mr. Si-Bok Yu. The M.S. thesis research topic and the grant research topic were one and the same. Several publications and conference presentations resulted or will result from the grant activities. These publications include the following:

- Yu, S., "Long-Term Aircraft Structural Integrity Prediction Under the Influence of Feedback Control," M.S. Thesis, Department of Aerospace Engineering, Old Dominion University, August, 1999.

- Yu, S., "Long-Term Aircraft Structural Integrity Prediction Under the Influence of Feedback Control," AIAA Mid-Atlantic Region I Student Conference, University of Virginia, Charlottesville, Virginia, April, 1999.

- Newman, B. and Yu. S., "Control of Crack Growth in a Flexible Aircraft," Proceedings of the CEAS/AIAA/ICASE/NASA Langley International Forum on Aeroelasticity and Structural Dynamics, Williamsburg, Virginia, June, 1999.

- Newman, B. and Yu. S., "Control of Crack Growth in a Flexible Aircraft," Proceedings of the AIAA Guidance, Navigation and Control Conference, Denver, Colorado, August, 2000.

Presented at the AIAA Mid-Atlantic Region I Student Conference, April, 1999.

Long-Term Aircraft Structural Integrity Prediction Under The Influence of Feedback Control

Sibok Yu

Masters Candidate
Department of Aerospace Engineering
Old Dominion University

The objectives of this research are to investigate and/or assess the influence of feedback control on fatigue damage reduction and long-term structural integrity of aircraft structural components. Repetitive stress load cycles such as during nominal cruise and less frequent but higher-stress transient loads originating from maneuvering flight and atmospheric gusts excite the aircraft. Micro-material imperfections in the structure such as cracks and debonded laminates, expand and grow in this environment, reducing the structural integrity and shortening the life of the airframe. Fatigue crack growth behavior predicted by a state space simulation under laboratory specimen loading indicated two significant factors for influencing crack growth (overload rate and overload period). A flexible airplane model was presented to explore the influence control systems, and other possible factors, may have on structural life extension. Four factors including mean stress, control system presence, control gain variation, and overload stress, were determined to be significant. Mean stress and control system presence are variable which cannot be altered by the designer. However, control gains and overload stress can be influenced. These latter factors can be modified to extend the life of the structures, and this implies a potential for new control logic to possibly enhance the structural life even further. Development of such new control logic will be investigated in future work.

I. Introduction

Over the operational lifetime of both military and civil aircraft, structural components

are exposed to hundreds of thousands of low-stress repetitive load cycles and less frequent but higher-stress transient loads originating from both maneuvering flight and atmospheric gusts.[1] State of the art, high-volume industrial processing has not yet reached a level where micro-material imperfections such as cracks and debonded laminates, are sufficiently absent within new aircraft structures. Under the flight loading environment, these imperfections expand and grow leading to a weakened structural system. References 2-7 provide a summary of common practices and newer methodologies for modeling and predicting the fracture mechanics of such systems. As an airframe fleet approaches the end of its useful structural life, two options are available for continued operations include refurbishment of critical load-bearing components or altogether reinventoring the fleet with newer models. Neither option is very attractive. Refurbishment is an intensive process requiring tear-down and build-up of internal structure not easily accessed and leads to large investments in labor, time and money. Reinventoring is also highly expensive requiring large amounts of direct capital.

One area having significant potential for reduction of crack growth and fatigue damage, and structural life extension, is flight control. To modify the airframe response dynamics arising from command inputs and gust disturbances, feedback loops are routinely applied to vehicles.[10,11] A dexterous flight control system architecture senses key vehicle motions and generates critical forces and moments at multiple points distributed throughout the airframe to elicit the desired motion characteristics. In principle, these same control loops can be utilized to influence the level of exposure to harmful loads impacting structural components during flight.

The objective of this thesis is to investigate and/or assess the leverage generated by flight control system feedback loops for reducing fatigue damage and enhancing

long-term structural integrity. Further, the study does not attempt to re-design the control architecture to maximize leverage, only the baseline control architecture parameters are varied. These higher fidelity models and control optimizations lie outside the scope of an initial investigation.

II. Analytic Crack Growth Model and Behavior

A simple load case in laboratory test, called short term, is illustrated in Figure 1. Here, σ_{min} , representing mean load for the specimen, is applied at the beginning, and σ_{max1} , low-stress repetitive load is applied to the specimen as described in Figure 2. This process is called 1 cycle, and this process is continued for N_1 times. After N_1 cycles, σ_{max2} replaces σ_{max1} for N_2 times, which is usually 1. Finally, σ_{max3} is applied for N_3 times. From Ref. 7, the analytic space state model describing crack growth within the specimen depicted in Figure 2 can be written as

$$\frac{dC}{dN} = \{ C_1 \{ F (\sigma_{max} - \sigma_0) \sqrt{\pi C} \}^m \quad \text{for} \quad \sigma_{max} \geq \sigma_0 \qquad (1)$$

$$\frac{dC}{dN} = 0 \quad \text{for} \quad \sigma_{max} < \sigma_0 \qquad (2)$$

where crack opening stress, $\sigma_o = f(R, \sigma_{max}, t)$. R denotes $\frac{\sigma_{min}}{\sigma_{max}}$. C denotes crack length, and the rate of crack growth, $\frac{dC}{dN}$, indicates the crack growth in each cycle.

Crack growth for a simple load case is given in Figure 3. Figure 3 illustrates highly non-linear behavior of crack growth, so the prediction of the crack growth is not possible before the simulation. As described in equation (2.1), the value of $\sigma_{max} - \sigma_0$ is directly related to the rate of crack growth. This non-linear behavior can be understood by studying σ_0 behavior shown in Figure 4. In this figure, σ_0 keeps low value until a

big stress is loaded to the specimen, σ_{max2}, at 17,000 [*cyc*]. This low σ_0 value occurs positive value of $\sigma_{max} - \sigma_0$, and makes continuous crack growing. Overload, σ_{max2} (compare to σ_{max1}) at 17,001 [*cyc*] results sudden increase of σ_0, and σ_0 keeps high value for about 15,000 [*cyc*] with small decrement. In this period, σ_0 is greater than σ_{max3}, so $\frac{dC}{dN}$ is equal to zero by equation (2). This zero rate of crack growth period corresponds to the flat line in Figure 3. When σ_{max3} is continuously applied, σ_0 drops suddenly, and σ_{max3} becomes greater than σ_0. Therefore, crack grows continuously until the specimen tsars off. The flat region is appeared because σ_0 suddenly increased, and the sudden increase of σ_0 has the physical meaning of sudden increasement of plastic area. In this flat period, the plastic area around crack keeps absorbing the stress. The plastic area shows sudden increasement when σ_{max}^{n-1} ($n-1$ th σ_{max}) is much smaller than σ_{max}^{n}.

Short Term Load Case

In reality, both high and low level stress will be loaded randomly. Before start to deal with the random loading, short term laboratory test is exercised to generalize the crack growth behavior. Investigated variables in this section are σ_{min} and three σ_{max}'s (σ_{max1}, σ_{max2}, and σ_{max3}). Other variables for short term load case in governing equation, equation (1), are either geometric factors or functions of σ_{min} and three σ_{max}'s. To investigate each of four variables, only one variable was varied in each cases.

First, for σ_{max1} and σ_{max3}, the higher stress directly result faster crack growth as shown in Figure 5~6. Second, crack growth with σ_{max2} variable in Figure 7 shows that the minimal σ_{max2} does not correspond to the minimal crack growth, and the result also

implies the existence of a optimal value of σ_{max2} for the maximum life of the structure. As described in Figure 7, for moderate value of overload (70~280), the crack growth is retarded as σ_{max2} is increased. However, for larger value of σ_{max2} (455~525), the material is torn and the crack growth shows a rapid increase, so crack reaches to C_{final} rapidly as σ_{max2} is increased. Approximately 385 [*MPa*] correspond to the minimal crack length ($\frac{\sigma_{max2}}{\sigma_{max1}} = 5.5$). Third, the larger value of $\sigma_{max} - \sigma_{min}$ ($\sigma_{max} > \sigma_{min}$ is assumed) correspond to the fast crack growing as shown in Figure 8.

These crack growth behavior show two points. One is the existence of an optimal value of σ_{max2}. The other is smaller $(\sigma_{max} - \sigma_{min})$ results in the larger life of the airframe.

Long Term Load Case

Long term case more representative of a long-term aircraft application is illustrated in Figure 9. Similar to the short-term load case, a repetitive load of strength σ_{max} is applied for N_1 cycles. Next, a over load, σ_{max2} , is applied for one cycle , N_2=1. This overload sequence is repeated continuously. Figure 10 shows the influence of σ_{max2} to the crack growth. The fastest failure occurred at the lowest value of overload stress σ_{max2}, but higher strength of overload stress shows longer life until σ_{max2} reaches to 160 [*MPa*]. When σ_{max2} is above 160 [*MPa*], the higher σ_{max2} corresponds to the faster failure. The overload rate ($\frac{\sigma_{max2}}{\sigma_{max2}}$) for the minimal crack length was just beyond 2. Overload rate above and below the value leads to larger crack length. The structural life summary graph, Figure 11, is generated to illustrate the number of cycles to the failure crack length at each overload rate. The graph has log scale on vertical axis which is representing the failure cycle. If the aircraft structure is loaded by the optimal overload

rate, the life of the structure will be significantly enhanced compare to non-optimal loaded structure. Experimental evidence is offered in Figure 12 to verify this result. In this figure, S_{ol} denotes σ_{max2}, and S_{max} denotes normal stress, σ_{max1}. The experimental result shows the optimal σ_{max2} at around 2. Overload period, N_1, for Figure 12 was 2,500 cycles.

After a number of simulations with the long-term crack model, one more interesting variable showed up. Different optimal overload rate was given by different overload period, N_1. Figure 13.a~d show the behavior of the optimal overload rate due to different N_1.

Summary of Short-Term and Long-term Crack Growth Behavior

In short term crack model simulation showed two points. First, there is an optimal value of σ_{max2}. Second, the smaller $\sigma_{max} - \sigma_{min}$ (when $\sigma_{max} > \sigma_{min}$) value results the longer life of the structure. Long term load case had two interesting results. First, there is an optimal value of $\frac{\sigma_{max2}}{\sigma_{max1}}$. Second, $\frac{\sigma_{max2}}{\sigma_{max1}}$ varies with N_1.

III. Flexible Aircraft Dynamics and Behavior

Flexible Airplane Model

In order to apply the crack growth behavior, a flexible airplane model is provided as an aircraft model. Modified B-1, Lancer, was chosen as a representative of high speed flexible airplane model as well as the reason of availability. Although non-linear data is available, linear longitudinal model will be offered for convenience. Assumed flight condition was set at 5,000 ft altitude and M. 0.6 flight speed. The bare airframe has stable open-loop response. The airplane model states can be derived by following two

equations.

State equation,

$$\dot{\vec{X}} = A\vec{X} + B\vec{U} \qquad (3)$$

and measurement equation,

$$\vec{Y} = C\vec{X} + D\vec{U} \qquad (4)$$

Constants, A, B, C, and D, are representing the aircraft characteristics. $\vec{X}$ is a vector consisted of state variables as following.

$$\vec{X} = [\ u,\ \alpha,\ \theta,\ q,\ \eta_1,\ \dot{\eta}_1,\ \eta_2,\ \dot{\eta}_2,\ \eta_3,\ \dot{\eta}_3,\ \eta_4,\ \dot{\eta}_4\ ]^T \qquad (5)$$

here, u denotes aircraft speed, α describes angle of attack, θ represents pitch angle. q describes pitch rate, i.e. $\dot{\theta}$, η_i denotes principal coordinate in each of i' th mode. This model shows 4 aeroelastic modes. Input vector, $\vec{U}$ can be denoted as following,

$$\vec{U} = [\ \delta_e,\ \delta_c\ ,\delta_f,\ \theta_{th},\ u_g,\ \alpha_g\ ]^T \qquad (6)$$

Input vector has six inputs. δ_e denotes elevator deflection, δ_c represents canard deflection, and δ_f denotes flap deflection. Throttle input was denoted by θ_{th}, and u_g and α_g represent gust velocity and gust angle. $\vec{Y}$ can be consisted of most any interested variables in the system. Meanwhile, the elements of $\vec{Y}$ can de selected to provide variables for stress calculation. Stress equation was given as following

$$\sigma = -E \cdot x_2 \cdot \frac{d^2 z}{dx^2} \qquad (7)$$

where,

$$\frac{z^2(x,t)}{dx^2} = \sum_{i=1}^{4} \phi_i(x)'' \cdot \eta_i(t) \qquad (8)$$

Therefore, $\phi_i(x)''$, $\eta_i(t)$ are required to be included in $\vec{Y}$ to calculate stress.

Here, $\phi_i(x)$ denotes the second derivative of modal vector.

Control System Design

Elevator deflection δ_e and canard deflection δ_c will be considered as control inputs. The responses of interest are q_1, pitch response at the cockpit, and q_3, pitch rate measured at the middle of the fuselage. The twelfth order model can be derived from the vehicle space-state model.

A conventional design method was hired here, consisting of sequential single-loop closures, using root loci, and relying upon knowledge of the physics of the elastic aircraft for synthesis strategy. From Table 3.1, a 2×2 system is

Table 1. Elastic Aircraft Transfer Functions

$$\frac{q_3(s)}{\delta_e} = \frac{-4.09(s+2.82\pm13.01i)(s-0.14\pm11.98i)(s+0.36\pm11.00i)(s+0.12\pm4.88i)(s+0.323)(s+0.025)(s+7.99e^{-15})}{d(s)}$$

$$\frac{q_3(s)}{\delta_c} = \frac{0.66(s+3.35\pm12.99i)(s+0.18\pm11.83i)(s+0.34\pm11.00i)(s+0.98\pm9.17i)(s+0.30)(s+0.026)(s-1.45e^{-14})}{d(s)}$$

$$\frac{q_1(s)}{\delta_e} = \frac{15.76(s+2.70\pm12.71i)(s-0.30\pm12.54i)(s+0.36\pm11.00i)(s-2.92)(s+3.34)(s+0.16)(s+0.065)(s+2.86e^{-15})}{d(s)}$$

$$\frac{q_1(s)}{\delta_c} = \frac{22.18(s+2.56\pm13.12i)(s+0.36\pm10.99i)(s+0.25\pm10.70i)(s+0.60\pm2.70i)(s+0.072\pm0.039i)(s-2.64e^{-15})}{d(s)}$$

where,

$$d(s) = (s+2.56\pm13.05i)(s+0.36\pm11.00i)(s+0.22\pm10.78i)(s+0.44\pm6.01i)(s+.45\pm1.17i)(s+0.0085)(s+0.0018)$$

considered.

$$q_3(s) = g_{11}(s)\,\delta_e(s) + g_{12}(s)\,\delta_c(s) \qquad (9.a)$$

$$q_1(s) = g_{21}(s)\,\delta_e(s) + g_{22}(s)\,\delta_c(s) \qquad (9.b)$$

First, q_1 and δ_c is closed to improve the aeroelastic mode damping. Recall that q_1

and δ_c correspond to a colocated sensor and actuator pair near the cockpit. The control law $\delta_c = \delta_c' - k_{22}q_1$ yields,

$$q_3 = \left(g_{11} - \frac{k_{22}g_{12}g_{21}}{1+K_{22}g_{22}}\right)\delta_e + \left(g_{12} - \frac{k_{22}g_{22}g_{12}}{1+K_{22}g_{22}}\right)\delta_c' \qquad (10)$$

$$q_1 = \frac{g_{22}}{(1+k_{22}g_{22})}\delta_c' + \frac{g_{21}}{(1+k_{22}g_{22})}\delta_e \qquad (11)$$

Figure 14 shows the root locus plot for $1+k_{22}\left(\frac{n_{22}}{d(s)}\right)$, where n_{ij} and $d(s)$ are the numerator and denominator polynomials of g_{ij}. A gain of $k_{22}=0.05$ $rad/rad/s$ increases the aeroelastic mode damping by over 60% of the open-loop value.

Second, an elevator-to-canard crossfeed is now applied to reduce aeroelastic mode excitation from the elevator. Interconnecting "up canard" with "up elevator" will reduce aeroelastic mode deflections from the elevator because the fuselage mode shape is similar to the fundamental bending mode shape of a slender beam. From equation (11),

$$q_3 = \left(g_{11} - \frac{k_{22}g_{12}g_{21}}{1+K_{22}g_{22}}\right)\delta_e + \left(g_{12} - \frac{k_{22}g_{22}g_{12}}{1+K_{22}g_{22}}\right)\delta_c'$$

Substitute the crossfeed $\delta_c' = k_{cf}\delta_e$,

$$q_3 = \frac{g_{11}k_{22}(g_{22}g_{11} - g_{12}g_{21}) + g_{12}k_{cf}}{1+k_{22}g_{22}}\delta_e \qquad (12)$$

The numerator can be simplified with identity .[23]

$$det\,[G] \;=\; g_{11}g_{22} - g_{12}g_{21} \;=\; \frac{\psi_G d}{d^2} \;=\; \frac{\psi_G}{d} \qquad (13)$$

where G represents the plant transfer function matrix corresponding to equation (10) and ψ_G is the transmission zero polynomial corresponding to G :

$$\psi_G(s) \;=\; -89(s+0.081)(s+0.46) \qquad (14)$$

Substitution of ψ_G yields

$$q_3 = \frac{n_{11} + k_{22}\psi_G + n_{12}k_{cf}}{d + k_{22}n_{22}}\,\delta_e \qquad (15)$$

Note that the crossfeed has the effect of moving the zeros of the $\frac{q_3}{\delta_e}$ transfer function (with the $\frac{q_1}{\delta_c}$ loop closed) from $n_{11} + k_{22}\psi_G$ to n_{12}. Figure 15 shows the root locus for $1 + k_{cf}\frac{n_{12}}{n_{11} + k_{22}\psi_G}$. A gain of $k_{cf} = -2.0$ *rad/rad* result in almost perfect pole-zero cancellation for the aeroelastic dipole in the effective $\frac{q_3}{\delta_e}$ transfer function.

Finally, $\frac{q_3}{\delta_e}$ loop is closed to improve short-period damping. The control law $\delta_e = p\delta - k_{11}q_3$ can be substituted into equation (12),

$$q_3 = \frac{p[g_{11} + k_{22}(g_{11}g_{22} - g_{12}g_{21}) + k_{cf}g_{12}]}{1 + k_{22}g_{22} + k_{11}[g_{11} + k_{22}(g_{11}g_{22} - g_{12}g_{21}) + k_{cf}g_{12}]}\,\delta \qquad (16)$$

here, p denotes a gain on the pilot input δ. The root locus for $1 + \frac{k_{11}[n_{11} + k_{22}\psi_G + k_{cf}n_{12}]}{d + k_{22}n_{22}}$ is shown in Figure 16 with the final closed-loop pole locations for a gain of $k_{11} = -0.05$ *rad/rad/s*. A value of $p = 0.6$ *rad/rad* was chosen to adjust the closed-loop frequency response direct-current (DC) value to that of the open-loop system excited by the elevator.

After some block-diagram manipulations, the block diagram for this system can be described as in Figure 17. Significant improvement in stress response is achieved as shown in Figure 18~19. This is a result of improved closed-loop pole-zero cancellations (see Table 2), as desired in the conventional control synthesis, or the aeroelastic mode has been rendered undistributable from pilot input.

Table 2. Closed-Loop Transfer Functions

$$\frac{q_3(s)}{\delta} = \frac{-5.41(s+2.90\pm13.00i)(s-0.086\pm12.00i)(s+0.36\pm11.00i)(s+0.20\pm10.78i)(s+0.87\pm6.16i)(s+0.31)(s+0.025)(s+2.56e^{-16})}{d(s)}$$

$$\frac{q_1(s)}{\delta} = \frac{-28.61(s+2.68\pm13.31i)(s+0.36\pm11.00i)(s+0.20\pm10.18i)(s+0.087\pm9.26i)(s+1.19\pm4.79i)(s+0.087\pm0.023i)(s+6.13e^{-16})}{d(s)}$$

$$d(s) = (s+2.55\pm13.05i)(s-1.08\pm10.73i)(s+0.20\pm10.78i)(s+0.36\pm11.00i)(s+0.93\pm5.98)(s+0.64\pm1.11i)(s+0.010)(s+0.0014)$$

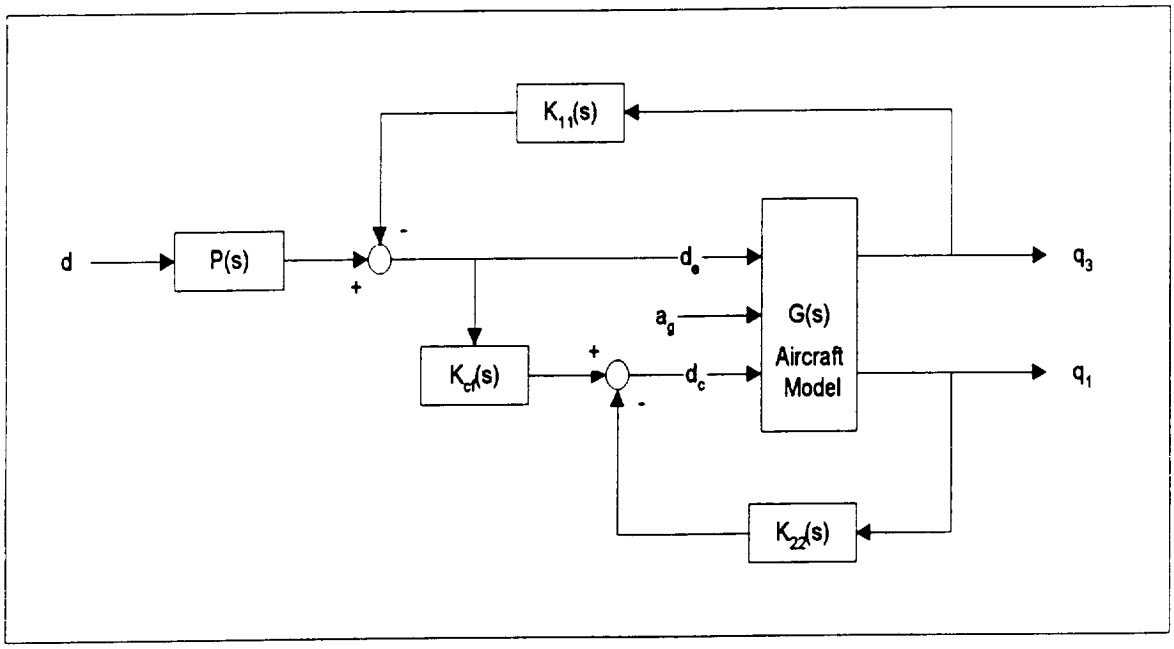

Figure 17. Classically designed Closed-Loop System

IV. Long-Term Structural Life of the Aircraft with Control System under Fatigue Crack Growth Problem

Development of Stress Input for Crack Model

An elevator maneuver can be represented by adding one positive deflection and another negative deflection as shown in Figure 20. This response is obtained by 1 ° step input for 1 *sec* followed by -1 ° step input for 1 *sec* based on the response of aircraft model

in section III. This positive and negative elevator deflection actually means altitude increment. Note that any points between two peak values has no effect to crack growth, so only peak points will be input for crack model. The strait line on the figure is connecting the peak points of the step response. Gust response obtained by 1 *ft/s* gust for 100 *sec* is also filterized as peak values to be the stress input of the crack model.

Although the aircraft is exposed to unpredictable random excitations in real environment, structural life prediction of airframe can be performed by some assumptions about the number of excitations and kind of excitations in each flight. Either 10 elevator maneuvers or 10 elevator maneuvers followed by one gust excitation is assumed to be the possible excitation during one flight. FAA (Federal Aviation Administration) refers that about 6.67 hours of flight can be estimated per one flight for B-747-400 airplane .[25] The same aircraft accumulated about 600 flight which corresponds to 600 set of either 10 elevator maneuvers or 10 elevator maneuvers followed by one gust per year. For life time scale prediction, the assumed maximum life of the specimen is set 5,000 flight which represents about 8.3 years of service.

Long-Term Crack Growth Characteristics

To investigate the influence of the control system, and to find out possible solutions to extend life of the structures under the fatigue crack problem by control system, long-term crack growth behavior excited by stress response in different conditions will be subject here.

i) Effect of Control System

First, the effect of the control system is provided in Figure 22. Three different inputs were applied to both open-loop system and closed-loop system, then the stress response was filterized to be the points of peak values of each cycles, and finally this peak

stresses excited the crack model to get the life-time scale crack growth behavior. First of all, the stress response excited by stick followed by gust input and only stick input are applied to the crack model, and the result is shown in Figure 22. The line which has lower crack growing rate corresponds to closed-loop for both input cases and two slightly different higher crack growth rate lines correspond to open-loop. For open-loop lines, the slightly higher line illustrates the crack growth for stick and gust combined input (case2 in Figure 21).

Significant extension of structural life is obtained by the control system. The crack growth of closed-loop system shows about 2 times of structural life compare to the open-loop result. This neglectable growth of crack may be caused by small gust input (1 *ft/s*), and several runs of this gust input response turned out that gust effect is no more neglectable when the gust is significantly greater than the given values here. Therefore, the influence of gust would be one of the subject of next investigation after this thesis work.

ii) Effect of Mean Stress

Effect of mean stress will be concentrated here. Note that the mean stress denotes the certain value of added stress to the dynamical stress response from section III. Mean stress represents the static stress of the specimen, and the value of static stress is strongly depend on '*y*' distance between the position of the specimen and the center of fuselage. Table 3^9 shows that the increased distance results the higher stress. Figure 23 shows the effect of mean stress to the crack growth. Note that the effect of mean stress is dominating the life of structures especially when σ_{nmi} is less than 60 $[MPa]$ ($\frac{\sigma_{nmi}}{\sigma_{\max}} < 0.75$; when $\sigma_{\max}$ denotes the maximum peak stress of the stress response).

iii) Effect of Control Gains

y [mm]	σ_z [N/mm^2]
381.0	302.4
352.0	279.4
269.5	213.9
145.8	115.7
0	0
-145.8	-115.7
-269.5	-213.9
-352.0	-279.4
-381.0	-302.4

Table 3. The Stress of the 100 [mm^2] Stringers
in Circular Cross-Sectional Fuselage
Under 200k [Nm] Bending Moment

The effect of control gains can be significantly important because it implies the possible life extension by adjusting control parameters. Also, this effect can be the basis of the new control system design to extend structural life which is the main subject of this thesis.

Recall about the gains of the control system, K_{11}, K_{cf}, and K_{22}. From Figure 17, relationship of inputs and outputs can be denoted as following.

$$\delta_e = -K_{11} q_3 + p\delta \quad , \tag{17}$$

and

$$\delta_c = -K_{22} q_1 + K_{cf}\, \delta_e \tag{18}$$

By substituting equation (17) to equation (18),

$$\delta_c = -K_{cf}\, K_{11} q_3 - K_{22} q_1 + -K_{cf} p\delta \tag{19}$$

Combining equation (17) and (19),

$$\begin{bmatrix}\delta_e\\ \delta_c\end{bmatrix} = -\begin{bmatrix}K_{11} & 0\\ K_{cf}K_{11} & K_{22}\end{bmatrix}\begin{bmatrix}q_3\\ q_1\end{bmatrix} + \begin{bmatrix}P(s)\\ K_{cf}P(s)\end{bmatrix}\delta \qquad (20)$$

Now, the gain matrix, K, and the gain from q_3 to δ_c, K_{21}, can be introduced for convenient.

$$K = \begin{bmatrix}K_{11} & 0\\ K_{21} & K_{22}\end{bmatrix} = \begin{bmatrix}K_{11} & 0\\ K_{11}K_{cf} & K_{22}\end{bmatrix} \qquad (21)$$

where, $K_{21} = K_{cf}K_{11}$. The crack growth behavior with each of K_{11}, K_{21}, and K_{22} variable are provided in Figure 23.a~c. The graph shows that K_{22} is the most sensitive gain in the control system. In addition, this results points that 40 % increase of the gain K_{22} extended about 18 % (about 700 flight) of the structural life which can represent 1.2 year of service.

Therefore, there is a possible solution to design a revolutionary control system which controls the aircraft to extend the life of the airframe. Optimizing the gain values is discovered to be one of methods here.

iv) Effect of Overload Stress

The effect of overload stress was already turned out to be significant in section II. Recall that the maximum life of the structure is the function of overload rate and overload period as the results of section II. This overload stress represents a stiff maneuver in each flight.

Crack growth under various overload rate is shown in Figure 24. Different overload stress was applied every 10 elevator maneuvers (every flight). Marked numbers on the line in Figure 4.11 indicates the corresponding overload rate of the line. The overload rate about 1.4 corresponds to the maximum life. This crack growth behavior basically

shows the same behavior with the long-term laboratory test result in section II, so the structural life summary chart can be also drawn here as Figure 25, when overload rate (N_1) is 20 flight. Observation of the Figure 25 infers that the life of structures in this summary figure shows almost coincident behavior with the long-term laboratory simulation in section II.

As section II, it turned out that the life of structure is also the function of overload period, N_1 . The summary chart excited by different overload rate and various overload period will be followed. Figure 26.a corresponds open-loop result, and Figure 27.b represents closed-loop result. These results prove that life of the structure is significantly effected by overload rate and overload period.

Summary of Long-Term Crack Growth Characteristics

The long-term crack growth behavior pointed out following four characteristics. First, flight control system significantly extend the life of the structures because the control system decreases the peak stress values, and generates smooth stress responses. Second, mean stress which represents the static load have dominative effect until the mean stress becomes close to the maximum stress, in contrast, when the mean stress gets significantly larger than the maximum stress, the effect becomes smaller. Third, the crack growth behavior with different gain values shows the potential to control life of the structure by the control system. At last, overload stress have dominative effect to the life of the airframe, the result also shows that the overload rate and the overload period are two governing factors in long-term fatigue crack growth phenomenon.

V. Conclusion

The short term laboratory test and the long-term aircraft model simulation under fatigue

crack growth pointed out several governing factors. In the point of controllability of the life of the structures, these factors can be divided by two. The value of nominal stress turned out to be the significant factor to the crack growth, but this factor is not controllable because the nominal stress is a dependent of position in the airframe. Existence of control system showed clearly extended the structural life, but this is not controllable either. Control gains, overload rate, and overload period are also dominating the life of the airframe, and these factors are controllable.

Optimization of gain values can be one solution of the life extension. With considering about the stability, trade between the extended life and the stability will be one of the potential future works. In addition, possible other effects of this trade need to be investigated. Effect of overload stress can be the most important factor in the point of the structural life control. Two dominating factors, overload rate and overload period, can be controlled a developed control system. Under the requirement of a certain maneuver, it is possible to achieve a desired movement of the aircraft or redistribution of stress. For example, a roll maneuver can be performed by either higher (or less) deflection of ailerons in different settling time or smaller deflection of ailerons with releasing flap in the same settling time. This kind of control surface redistribution or desired reaction of the control surfaces derive the future research to the new control system which can control the life of the airframe, and the stress response under gust input can also be reorganized to be desirable by the new control system.

The new control system will include the function to increase or decrease the original stress response to the desired stress to be the optimal repetitive underload stress (σ_{max1}) and less frequent overload stress (σ_{max2}). Also, the new control system need to have the function to set the flight condition to the optimal overload period. The sacrifice of

performance by this new control system should be investigated and the trade between the longer life and the performance should be concerned in next research. The new control system can be applied to the aircraft without any other devices, and the control system might guarantee longer life and better safety of the airframe. The new controller can also be applied to the aircraft structure design. Once this life control system is confirmed to be reliable, the weight of the airframe can be reduced due to the efficiency of the life-control.

References

1. Lomax, T. L. *Structural Loads Analysis for Commercial Transport Aircraft : Theory and Practice*, American Institute of Aeronautics and Astronautics (AIAA)

2. Thomson, A. G. R. and Lambert, R. F., *Acoustic Fatigue Design Data Part I-IV*, AGARD (Advisory Group for Aerospace Research & Development), AGARD graph No. 162, January 1975.

3. Newman, J. C., Philips, E., and Everett, R. A., Jr. *Fatigue Life and Crack Growth Prediction Methodology*, NASA-TM-109044, October 1993.

4. Anderson, T. L., *Fracture Mechanics Fundamentals and Applications*, CRC Press, Boca Raton, Florida, 1995.

5. Newman, J. C., A *Crack Opening Stress Equation for Fatigue Crack Growth*, International Journal of Fracture, Vol. 24, No. #, 1984, pp. R131-R135.

6. Ibrahim, F. K., Thomson, J. C. and Topper, T. H., A *Study of the Effect*

of Mechanical Variables on Fatigue Crack Closure and Propagation, International Journal of Fracture, Vol. 8, No. 3, 1986, pp. 135-142.

7. Patankar, R., Ray, A. and Lakhtakia, A., *A State-Space Model of Fatigue Crack Dynamics*, International Journal of Fracture (to appear 1998)

8. Dawicke, David S., *Overload and Underload Effects on the Fatigue Crack Growth Behavior of the 2024-T3 Aluminum Alloy*, NAS1-96014, NASA (National Aeronautics and Space Administration), March, 1997.

9. T. H. G. Megson, *Aircraft Structures*, Edward Arnold, 1990.

10. Aviation Week & Space Technology, *FAA Directive Target Boeing 737s, 747s*, January 13, 1997.

11. Blakelock, J. H., *Automatic Control of Aircraft and Missile*, Wiley-Interscience, New York, New York, 1991.

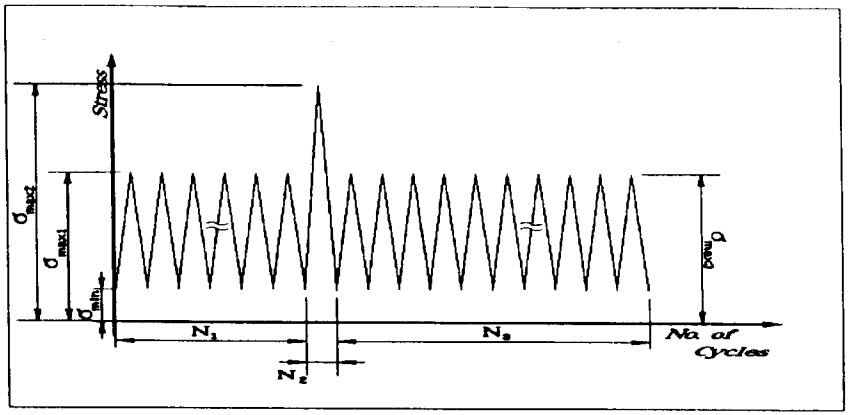

Figure 1. Applied Load for Short-term Load Case

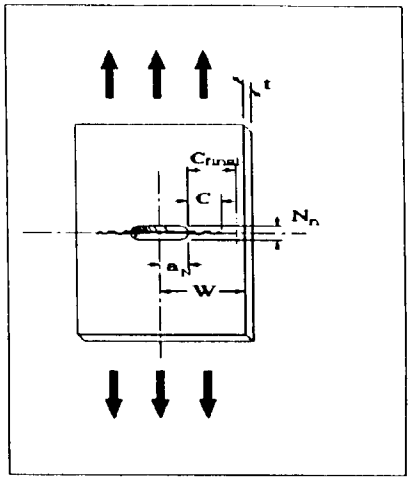

Figure 2. Specimen for Crack Growth Analysis

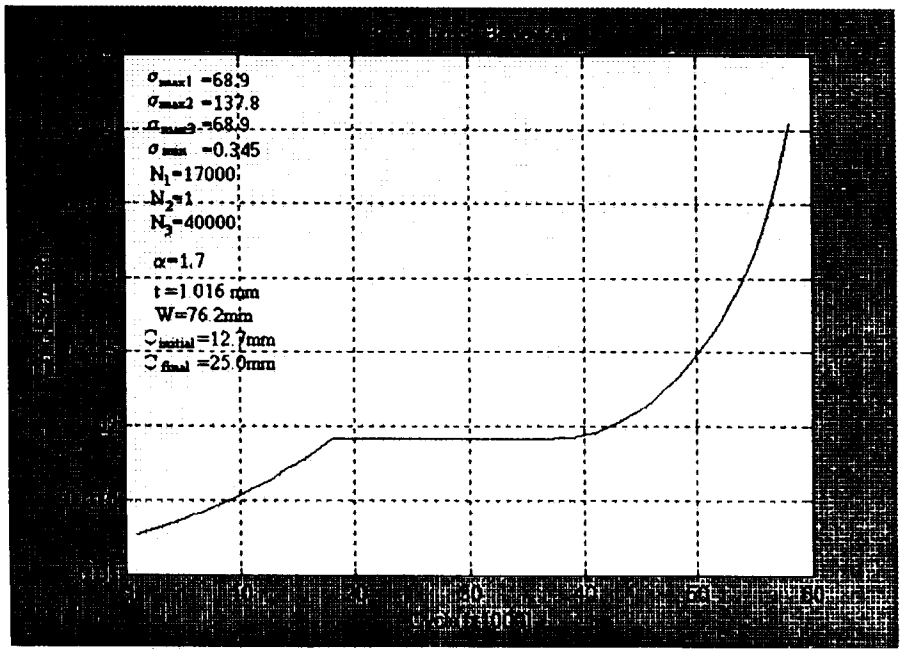

Figure 3. Basic Crack Growth Behavior ; $\sigma_2 = 137.8$ [*MPa*]

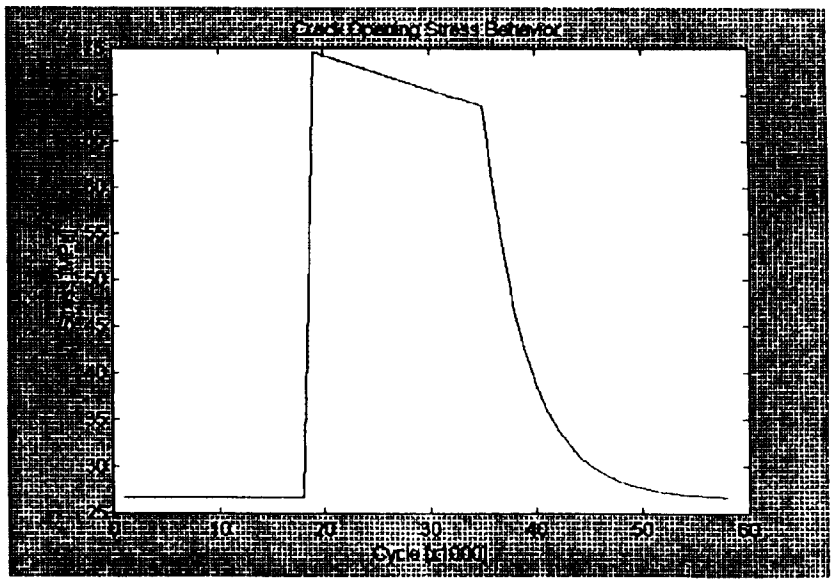

Figure 4. Behavior of Crack Opening Stress; σ_0

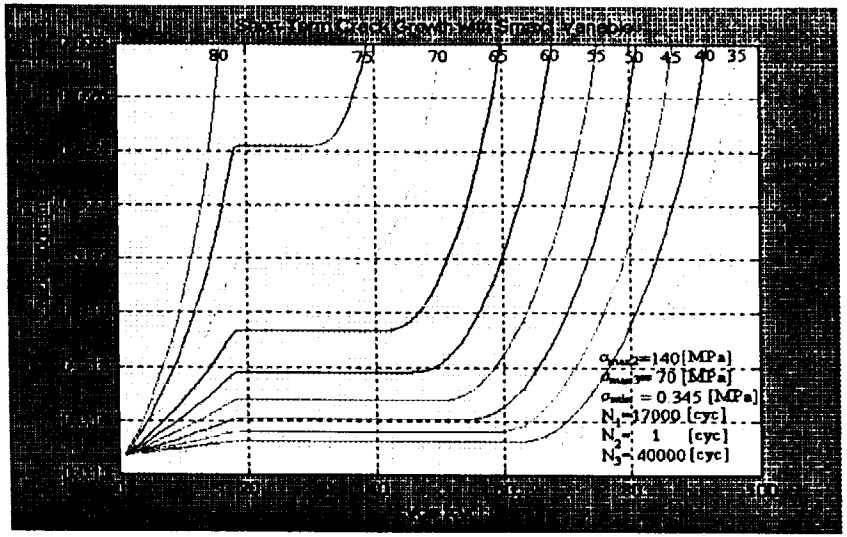

Figure 5. σ_{max1} Variable

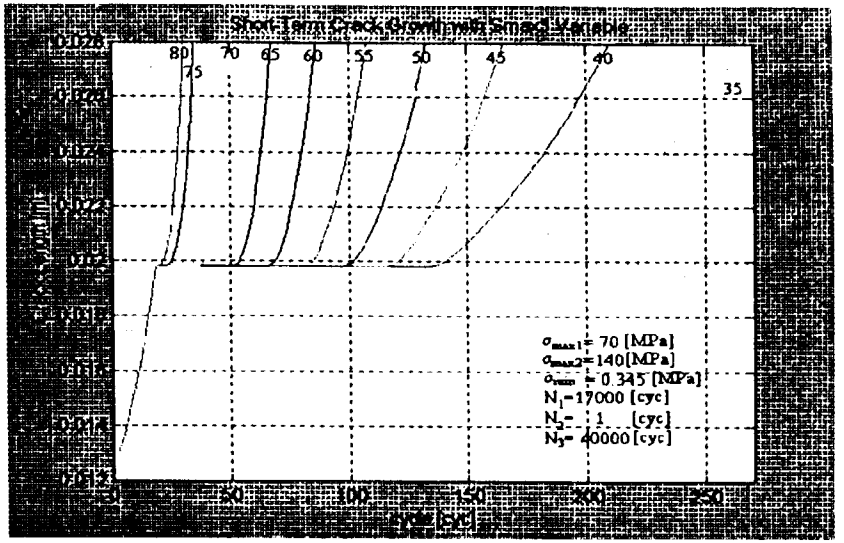

Figure 6. σ_{max3} Variable

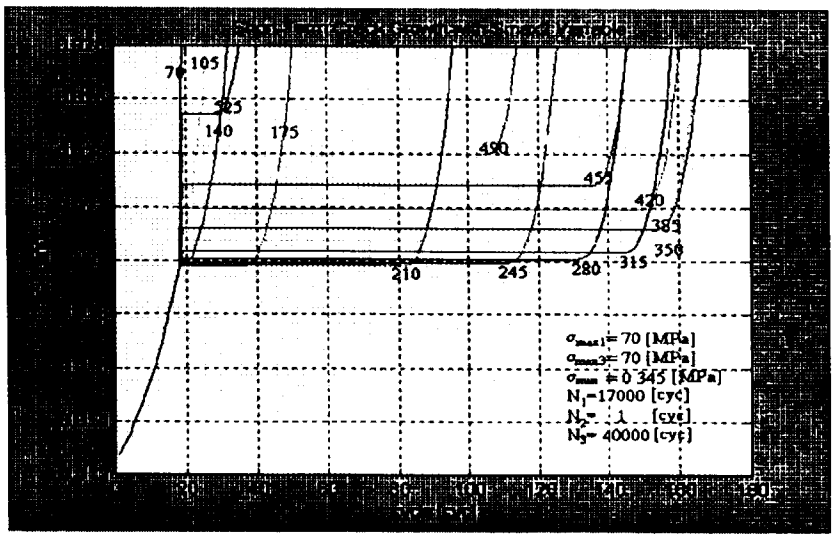

Figure 7. σ_{max2} Variable

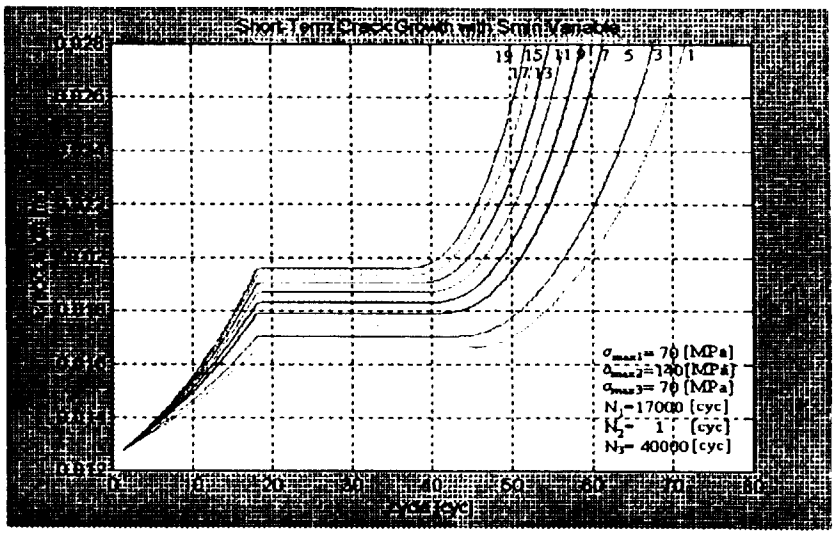

Figure 8. σ_{min} Variable

Figure 5 - 8. Short-Term Crack Growth Behavior

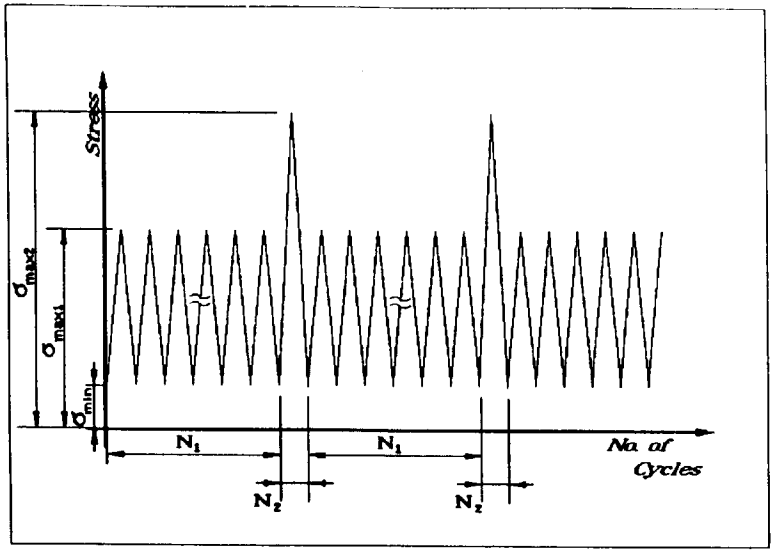

Figure 9. Applied Load for Long-term Load Case

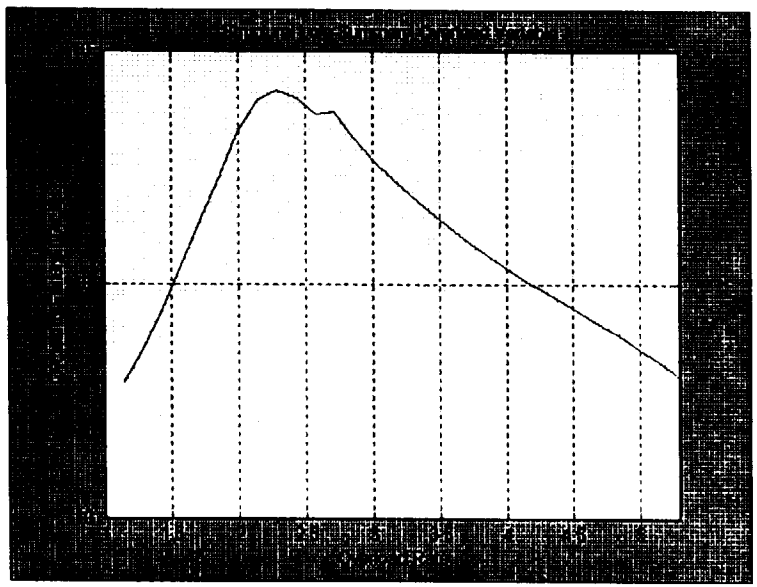

Figure 11. Structural Life Summary

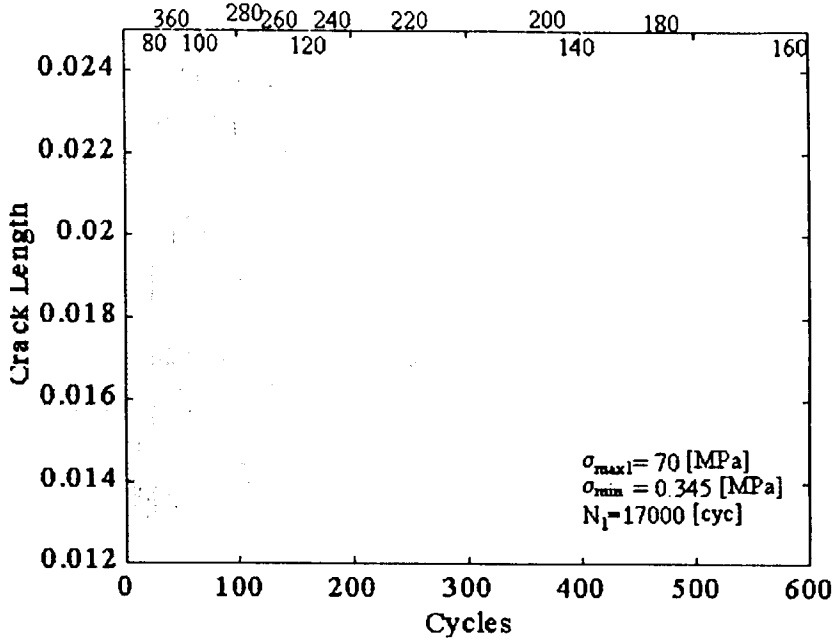

Figure 10. Long-Term Crack Growth Behavior - σ_{max2} variable

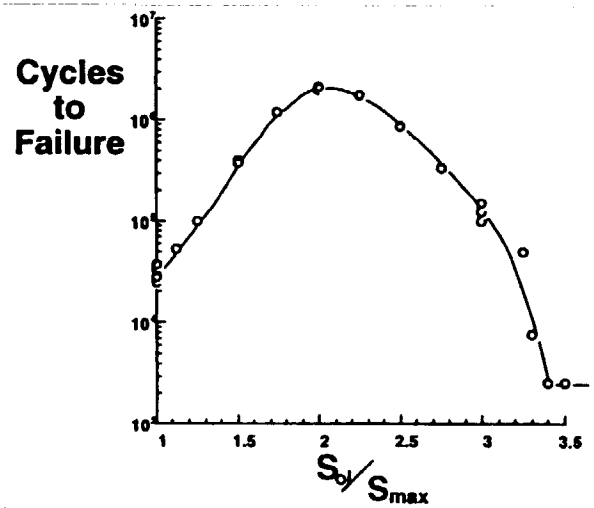

Figure 12. Experimental Result .[8]

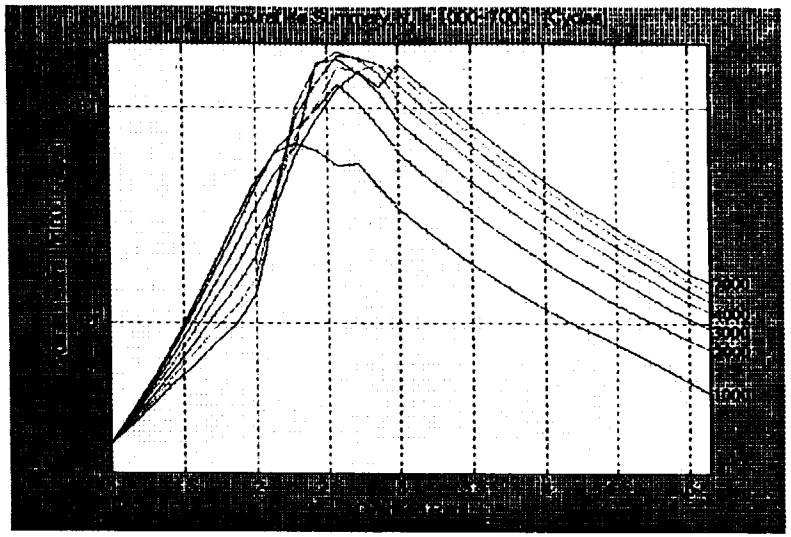

(a)

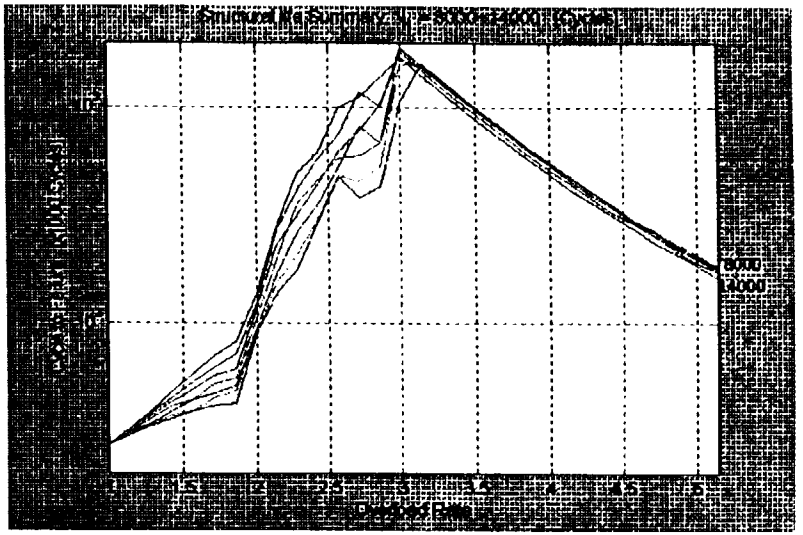

(b)

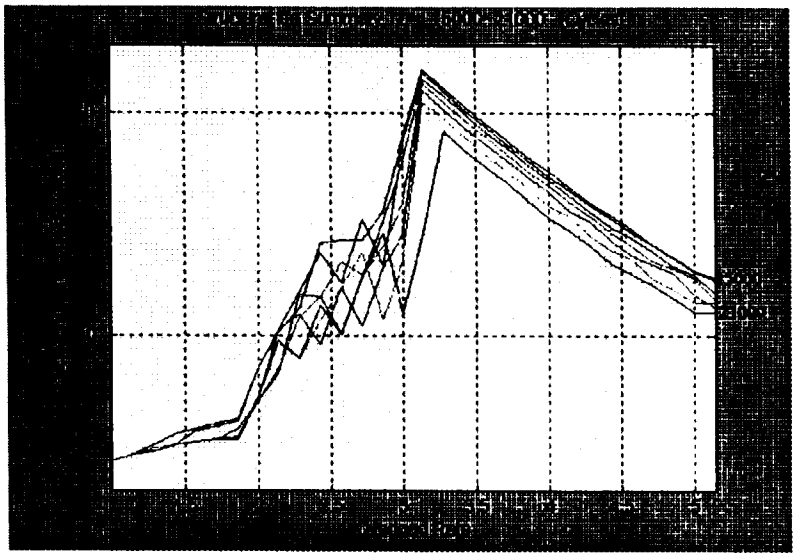

(c)

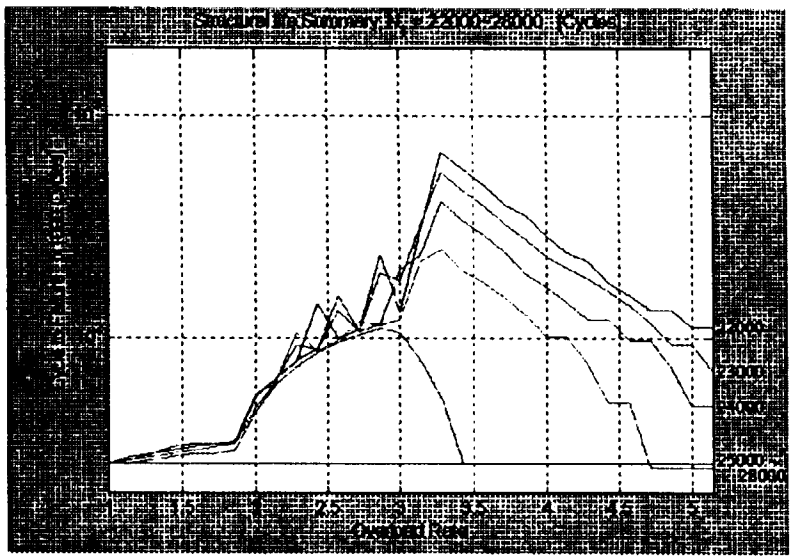

(d)

Figure 13 Structural Life Summary; N_1 and σ_{max2} Variable
; N_1 : 1,000 ~ 28,000 cycles σ_{max2} : 70 ~ 360 [*MPa*]

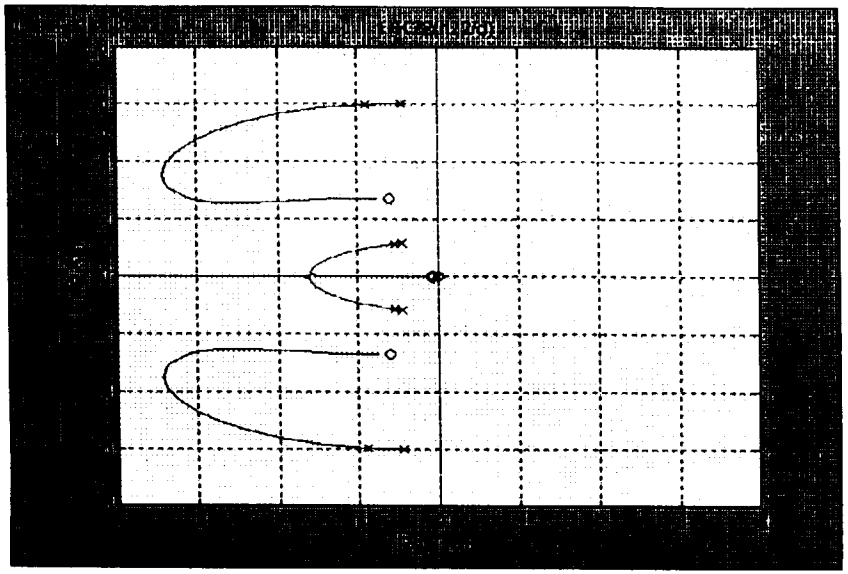

Figure 14. Cockpit Pitch Rate to Canard Root locus

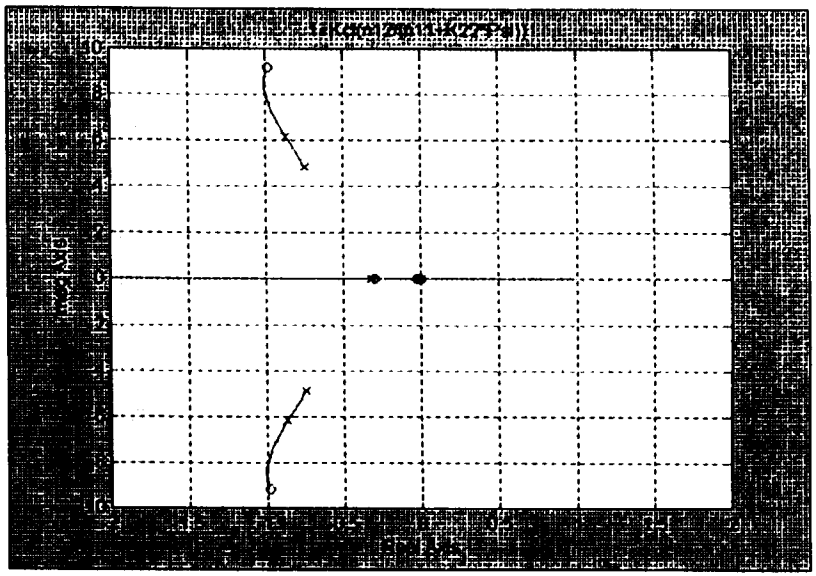

Figure 15. Elevator to Canard Root Locus

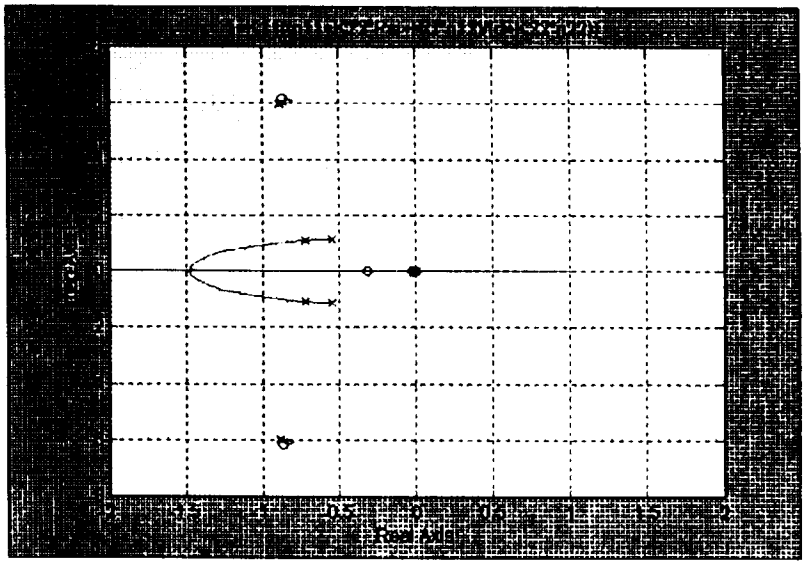

Figure 16. Center of Fuselage Pitch Rate to Elevator Root Locus

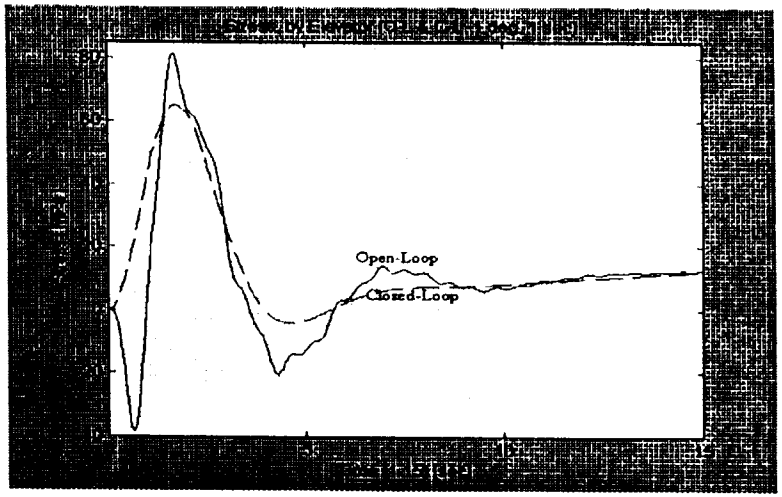

Figure 18. Elevator Step Response (1 sec, 1 °)

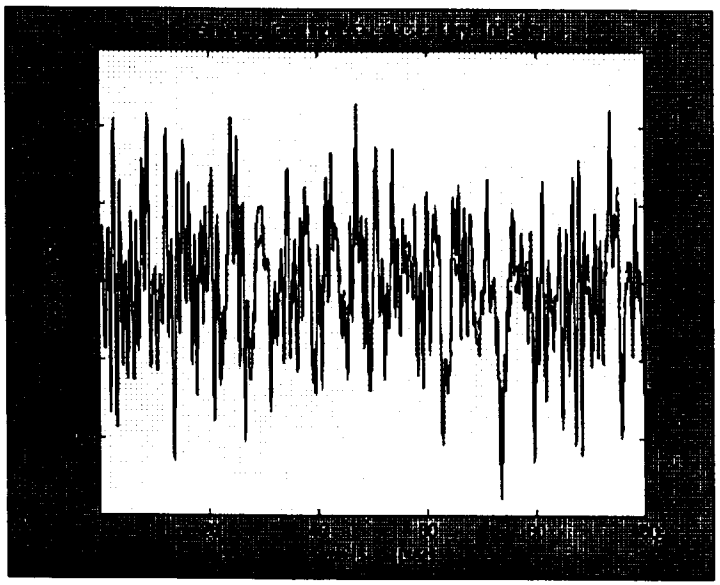

Figure 19.a. Gust Response (1 *ft/s*, 100 *sec)*

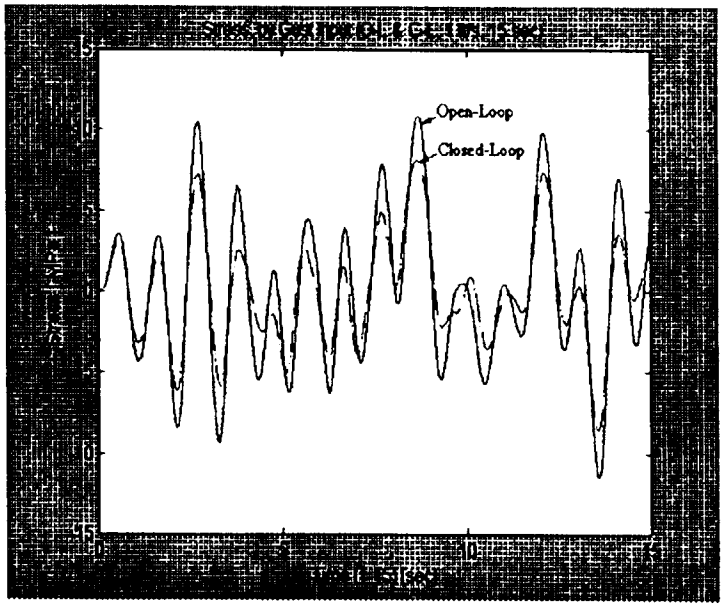

Figure 19.b. Zoomed Gust Response
(0 ~15 *sec* of 100 *sec)*

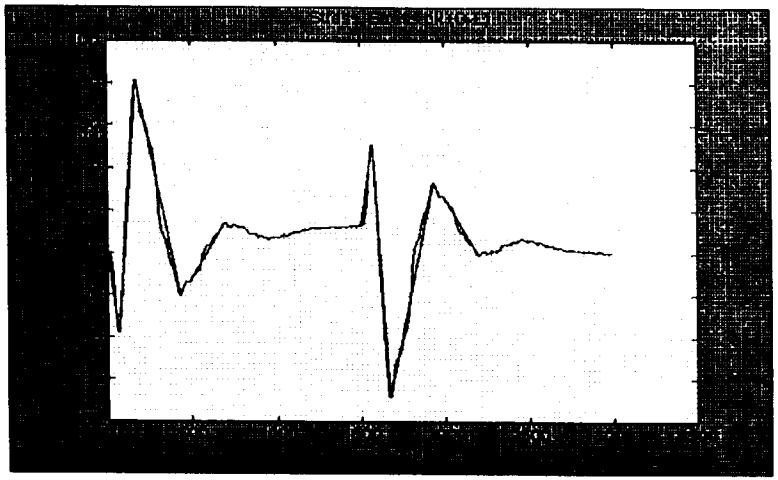

Figure 20. Positive and Negative Step Response Representing One Elevator Maneuver and Peak Stress for Crack Model

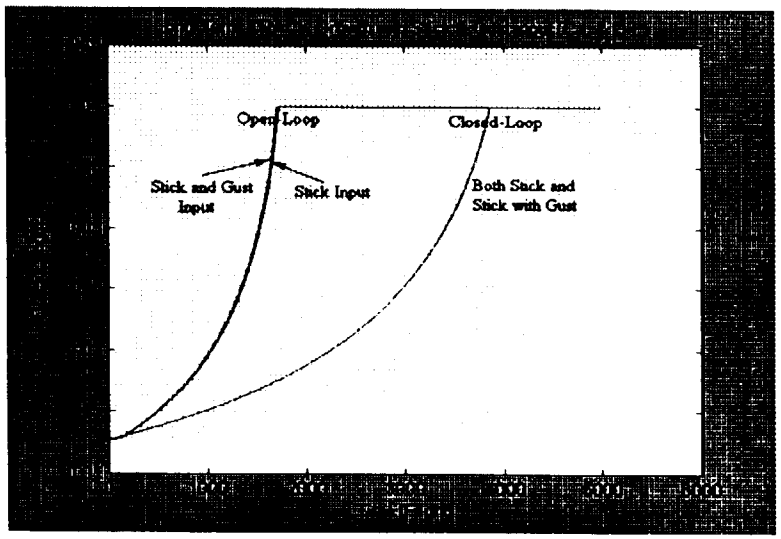

Figure 22. Crack Growth Graph by Stick and Gust or Only Stick Input for Open-loop and Closed-loop Comparison

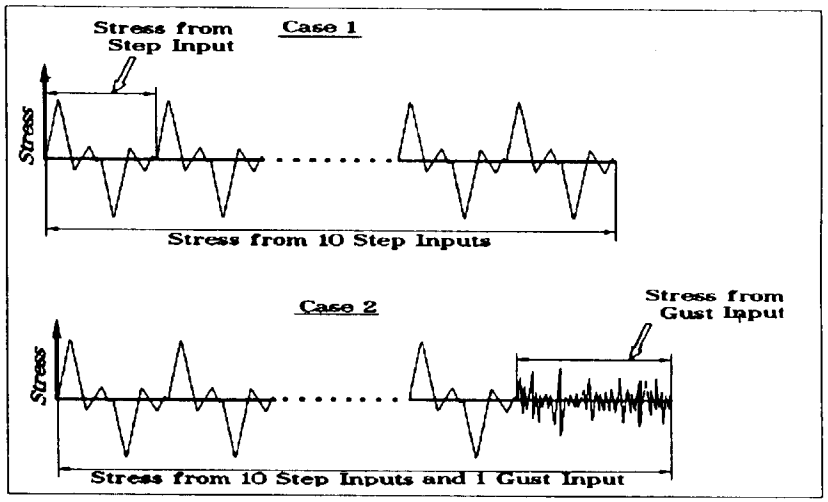

Figure 21. Two Cases of Maneuvers Representing One Flight

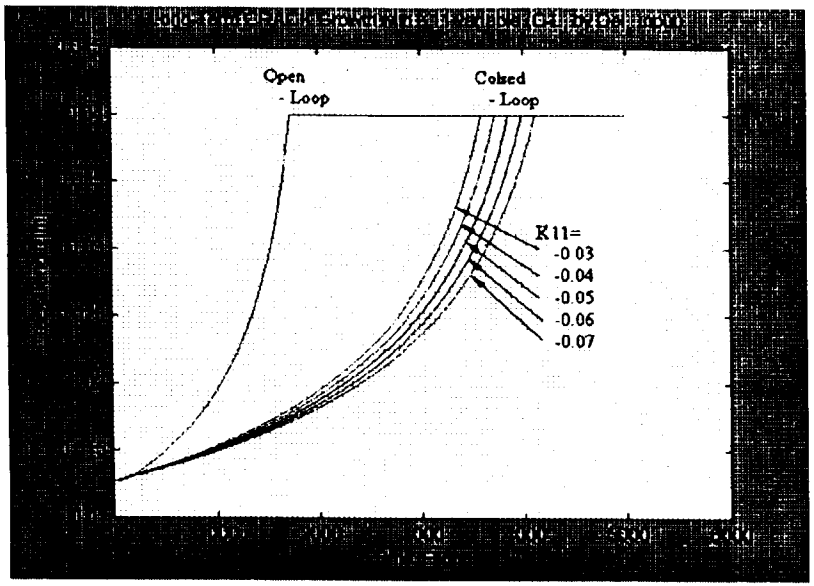

Figure 23.a. Effect of Control Gain, K_{11} , by Elevator Input.

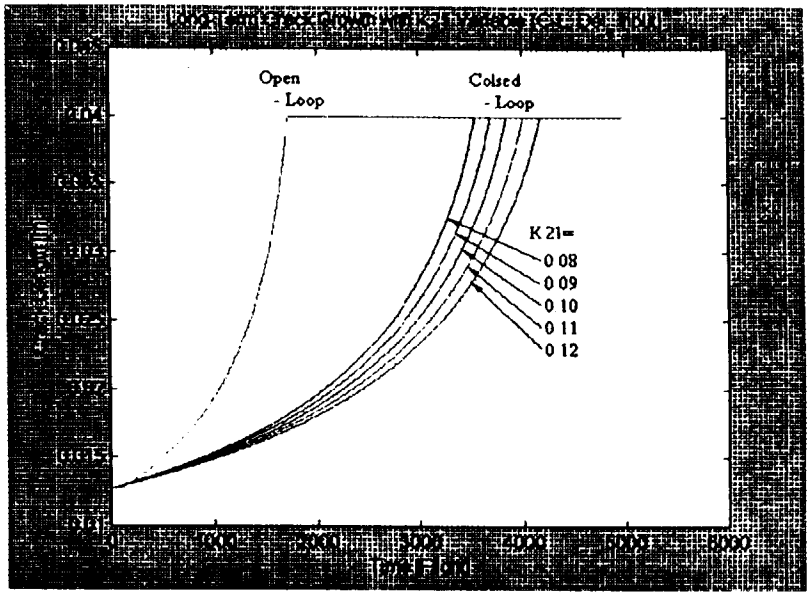

Figure 23.b. Effect of Control Gain, K_{21} , by Elevator Input.

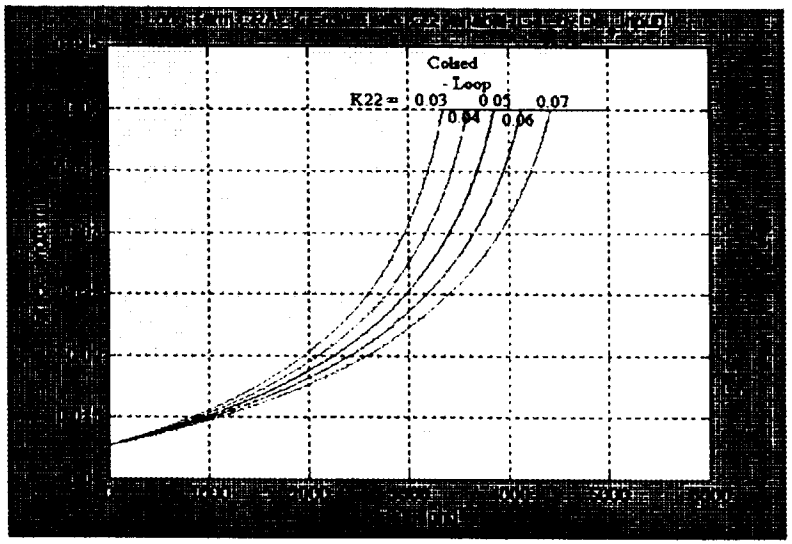

Figure 23.c. Effect of Control Gain, K_{22} , by Elevator Input.

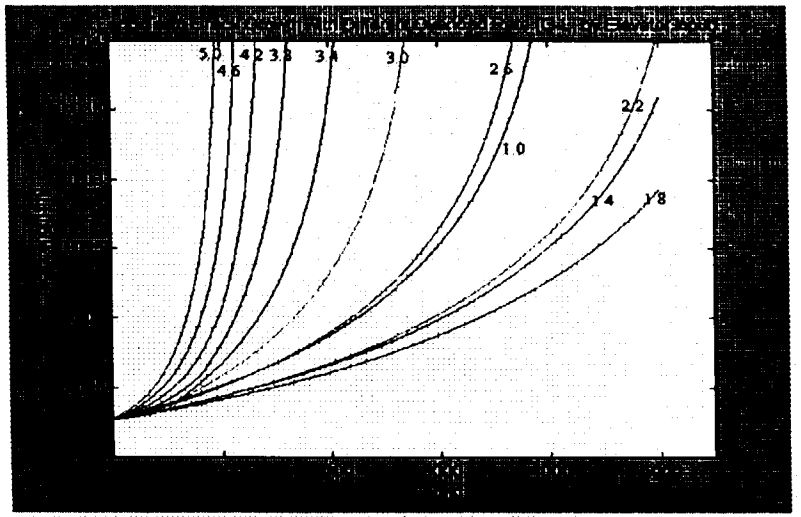

Figure 24. Long-Term Crack Growth with Overload Stress

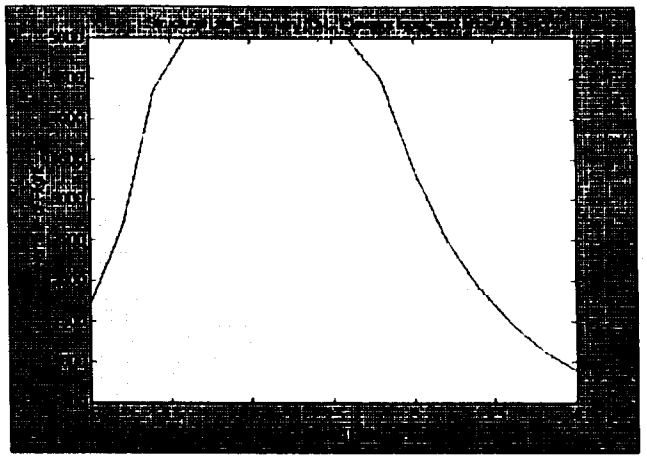

Figure 25. Structural Life Summary
(Open-Loop, $N_1 = 20$)

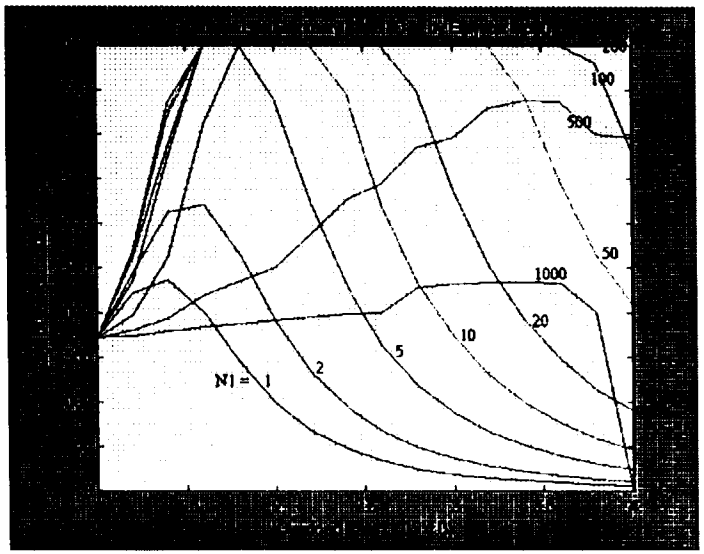

26.a. Open-Loop

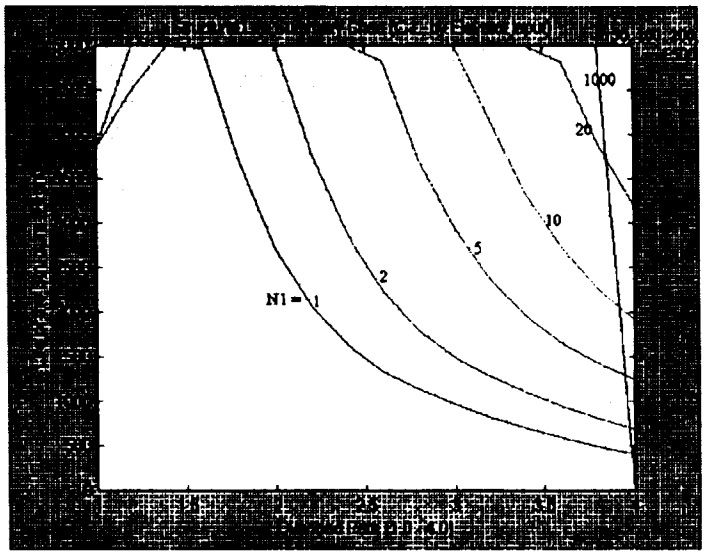

26.b. Closed-loop

Figure 26. Long-Term Crack Growth with Overload Rate and Overload Period Variable